

Numerical modeling of the labyrinth seal taking into account vibrations of the gas transmittal unit rotor in aeroelastic formulation

L.N. Butymova¹, V.Ya. Modorskii¹

¹Perm National Research Polytechnic University, pr. Komsomolsky 29, 614099, Perm, Russia

Abstract

The article deals with the issues related to the mutual influence of vibrations and gas dynamic processes in the labyrinth seals (LS) of gas transmittal unit compressors. The mutual influence of vibrational gas dynamic processes in LS and vibrations of the rotor is studied. Within the framework of the unified algorithm, a solution is obtained for an unsteady aeroelastic one-dimensional gas flow problem in a deformable LS. A new factor (the rotor diameter in the LS region), which affects the pulsation magnitude of the gas dynamic force in the LS, is revealed. Changing the diameter of the rotor, you can reduce vibration. In this case, it is possible to reduce the designated clearances in the LS and to reduce the leakage.

Keywords: aeroelasticity; rotor vibration; labyrinth seal; unified algorithm; stress; pressure; deformation; displacement

1. Introduction

To ensure a contactless connection between a rotating rotor and a stationary body in aircraft engines [16], high-pressure pumps [13, 14], etc., labyrinth seals (LS) are used. In seals of labyrinth type, the working medium is sealed by throttling it when moving through successively located constrictions and extensions.

The main task of the LS is to ensure tightness of the rotor, therefore expansions and constrictions of the flow in LS are usually considered in the direction parallel to the rotor axis. However, in order to ensure aerovibration resistance, it is necessary to take into account the processes of motion of the working medium that take place in the peripheral direction of the LS under the rotor vibrations. It should be noted that sequencing of the constrictions and expansions affects the oscillation amplitude in the gas-dynamic cavity between the LS and the rotor, and also increases the flow non-uniformity. Consequently, refusal to take these elements into account in aeroelastic calculation [15, 21-22] can give an additional margin from the point of view of reducing oscillations in LS, and, which is important for solving the related problems of continuum mechanics [19], reduce complexity and time of calculations.

Based on the said above, the LS calculation is replaced by calculating the gap seal, equivalent (with margin) to the labyrinth seal, if we consider the processes taking place in the LS circumferential direction.

As it is known, LS works at high temperatures and high rotation speeds. Under critical operating conditions the LS is effected by significant loads from the gas-dynamic flow as well as the LS influences the gas-dynamic flow. The impact of this process is ambiguous and requires more detailed research. Publications related to vibrational processes in LS and vibration of rotors, consider the influence of precession [11], geometric characteristics of LS [12] and in the most cases do not take into account the influence of gas-dynamic forces.

The gas dynamic processes that arise in LS at the rotor vibrations caused, for example, by technological imbalances, may lag behind the rotor oscillations. It is necessary to analyze the possibility of amplifying or weakening the rotor vibrations and dependence of these processes on the LS characteristics [9-10].

The classical formulation of the vibration problem takes into account the influence of structural [20], physical-mechanical and technological parameters on vibration, but does not consider the influence of gas dynamic loads.

When considering the problem of the vibration effect on gas-dynamic processes in the labyrinth seals of a centrifugal compressor model gas transmittal unit in a unidirectional dynamic related formulation it is possible to take into account the gas-dynamic factors [13, 17]. In addition, it becomes possible to calculate the oscillation parameters of gas-dynamic forces acting on the rotor [4-8].

2. Object of study

A physical model describing the LS operation in an aeroelastic formulation is developed. As a model, the LS scan with the width corresponding to the LS width is considered. In a unidirectional FSI-statement, the rotor motion is replaced by the movement of pistons located diametrically opposite, and moving with the specified amplitude and frequency (Fig.1). The scan length is equal to the circumference of the gas-dynamic cavity, which is aligned along the middle line between the rotating rotor and the stationary LS.

The model is quasi-two-dimensional, dynamic.

Thus, the rotor oscillations in the LS gap are modeled by a nonlinear dynamic quasi-two-dimensional gas dynamic scan model of the LS gap with movable boundaries. Extrusion of the gas as the gap is reduced and filling free volume with the gas as the gap is increased during the rotor oscillation in the LS is modeled by two pistons moving in harmonic order. Their oscillation frequency is the same and corresponds to the rotor oscillation frequency, calculated from the wave path equal to the length of the circumference arc around the rotor. The piston oscillation amplitudes are equal (formula 1). While calculating, the

oscillations of displacements, velocities, pressures and gas-dynamic force acting on the rotor in the LS area are recorded at the control points. The displacement of these oscillations (φ_U) may take place with respect to two parameters: the gas-dynamic forces acting on the rotor in the LS area and the rotor displacements. With different phases (φ_U) convergent, divergent and steady oscillatory processes can be observed.

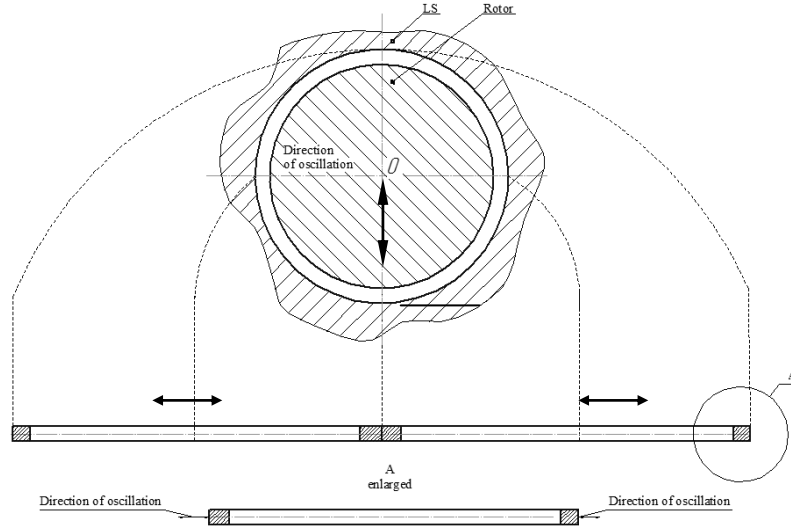


Fig. 1. Formation of the LS calculation scheme (unidirectional FSI-statement).

3. Mathematical model

The mathematical description of the gas-elastic process in this formulation includes the following relationships:

$$\frac{\partial \rho_{\Gamma}}{\partial t} + \frac{\partial \rho_{\Gamma} V_x}{\partial x} = 0 \quad (1)$$

$$\frac{\partial \rho_{\Gamma} V_{x\Gamma}}{\partial t} + \frac{\partial (\rho_{\Gamma} V_{x\Gamma} V_{x\Gamma})}{\partial x} + \frac{\partial P}{\partial x} = 0 \quad (2)$$

$$\frac{\partial \rho_{\Gamma} E}{\partial t} + \frac{\partial (\rho_{\Gamma} E V_{x\Gamma})}{\partial x} + \frac{\partial (P V_x)}{\partial x} = 0 \quad (3)$$

$$P = \rho_{\Gamma} (k-1) \left(E - V_{x\Gamma}^2 / 2 \right) \quad (4)$$

$$\frac{\partial \rho_K}{\partial t} + \frac{\partial (\rho_K V_{xK})}{\partial x} = 0 \quad (5)$$

$$\frac{\partial (\rho_K V_{xK})}{\partial t} - \frac{\partial \sigma_{xx}}{\partial x} = 0 \quad (6)$$

$$U_x = U_{x0} + \int_0^t V_{xK}(t) dt \quad (7)$$

$$\varepsilon_{xx} = \frac{\partial U_x}{\partial x} \quad (8)$$

$$\sigma_{xx} = E \varepsilon_{xx} \quad (9)$$

- initial conditions

at $t = 0$ (Gas):

$$P = P_0, \quad \rho_{\Gamma} = \rho_{0\Gamma}, \quad E = P_0 / \rho_{0\Gamma} (k-1) \quad (10)$$

at $t = 0$ (SSS):

$$\sigma_{xx} = 0, \quad \varepsilon_{xx} = 0, \quad U_{x0} = 0, \quad V_x = 0$$

Boundary conditions (SSS)

a) «rigid wall»

(«Sticking»)

$$V_{xK} = 0, \quad V_{x\Gamma} = 0, \quad (11)$$

a) gas-structure

$$\sigma_{xx} = -P_{TP} \quad V_{.xK} = V_{.xT}$$

The boundary condition for the piston motion:

$$V_{left.piston} = -V_0 \sin(\omega t); \quad V_{right.piston} = V_0 \sin(\omega t) \tag{12}$$

where V_0 – amplitude of the piston oscillations, ω – the piston oscillation frequency.

4. Method of solution

For solving gas dynamic tasks was used method of large particles. Using the same method for solving gas dynamic and stress-strain state tasks provide unity mesh for gas dynamic region and stress-strain state tasks. For this used unified system of differential equations to ensure coupled solving for elastic tasks and gas dynamic tasks. Thus we used method of large particles for calculations.

The main idea of method’s large particles consisted in splitting into physical processes of the initial non-stationary system of Euler equations which written in the form’s conservation laws. The space is modeled by particle system which coincides with cell’s Euler grid in the moment. If stationary solving is, we get it in process stabilized solving. So all process solving composed multiple repetitions of time steps.

Each computational cycle is divided into seven stages. The first three stages are designed to solve the gas dynamic tasks. The next four stages are designed to evaluate the parameters dynamic stress-strain state of the structure.

5. Description of results

5.1. Analysis of the influence of geometric characteristics

In a unidirectional aeroelastic formulation, the solution using equations (1-4) and initial and boundary conditions, yielded the following results.

When investigating the dependence of pressure fluctuations in the LS gas-dynamic cavity on the LS geometric characteristics the rotor diameters in the LS area varied and were equal to 65, 130, 195 or 260 mm. The working body of the gas-dynamic cavity is air, adiabatic exponent equals 1.4, density $\rho = 1,29 \text{ kg / m}^3$.

With an increase in the shaft diameter from 65mm to 260mm, the pressure oscillations in the gas-dynamic cavity are noted, which have a time periodic character (Fig. 2). The pressure amplitude is 101368.8 Pa with $D = 65\text{mm}$, with $D = 130 \text{ mm}$ the pressure amplitude is 148792.2 Pa, and with $D = 195\text{mm}$ the pressure amplitude is 107577.7 Pa, with $D = 260\text{mm}$ the pressure amplitude is 101732.1Pa.

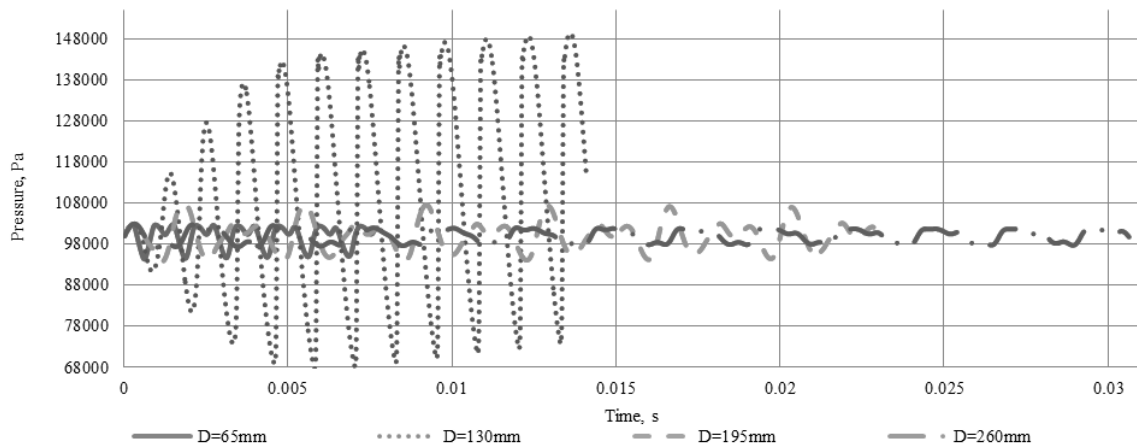


Fig. 2. Dependence of the gas dynamic pressure of the gap near LS on time at different geometric characteristics of LS.

Table 1. Pressure amplitude for LS different geometric characteristics.

Computational experiment	1	2	3	4
Rotor diameter D, mm	65	130	195	260
Maximum pressure amplitude U_p , MPa	0.1	0.15	0.11	0.102

When studying the dependence of the temperature oscillations in the gas-dynamic cavity on the geometric characteristics of the LU, the diameters of the rotor in the zone of the LU varied and assumed values of 65, 130, 195 or 260 mm, the working fluid of the gas-dynamic cavity is air, the adiabatic index is 1.4, $\rho = 1,29 \text{ kg/m}^3$.

With an increase in shaft diameter from 65mm to 260mm, oscillations in the temperature of the gas-dynamic cavity are noted, which have a periodic character of the change in time (Fig. 3). The temperature amplitude is 272.4936K. At $D = 65\text{mm}$,

at $D = 130\text{mm}$ the temperature amplitude is 323.6043K , and at $D = 195\text{mm}$ the temperature amplitude is 279.0668K , at $D = 260\text{mm}$ the temperature amplitude is 274.4728K

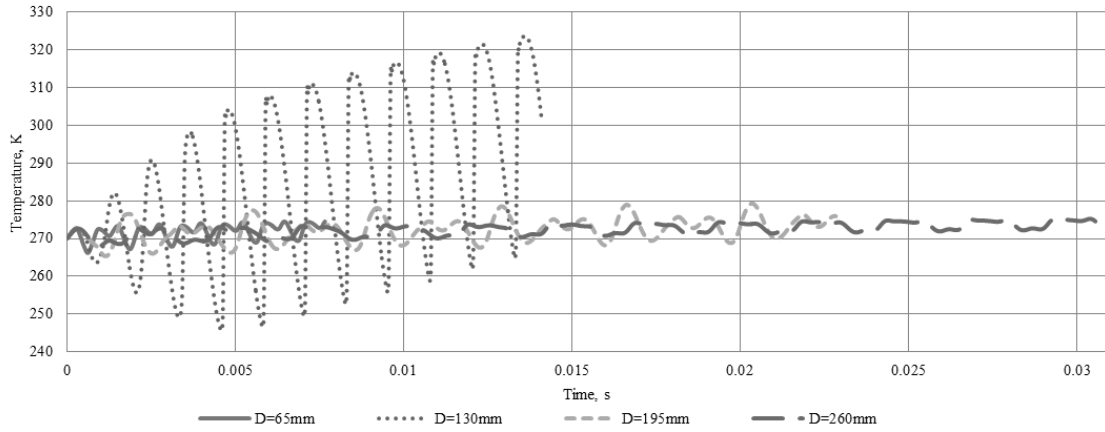


Fig.3. Dependence of the gas-dynamic gap temperature near LS on the time for LS different geometric characteristics.

Thus, when designing the LS it is necessary to take into account the geometric dimensions of the rotor and the gap between the rotor and the LS in order to reduce possible vibrations.

Table 2. Temperature amplitude for LS different geometric characteristics.

Computational experiment	1	2	3	4
Rotor diameter D , mm	65	130	195	260
Temperature amplitude U_T , K	272.4936	323.6043	279.0668	274.4728

5.2. Analysis of the influence of kinematic parameters

The dependence of pressure oscillations in the LS gas dynamic cavity on the kinematic parameters of propagation speed of gas oscillations in the circumferential direction varied and equaled 3.5, 7.0 or 10.5 m/s, the working fluid of the gas-dynamic cavity is air, the adiabatic index is 1.4, $\rho = 1, 29 \text{ kg/m}^3$.

With speed increase from 3.5 m/s to 10.5 m/s, the pressure oscillations of the gas-dynamic cavity are noted, which have a periodic character (Fig. 4). The pressure amplitude is 100918.3 Pa at $V = 3.5 \text{ m/s}$. At $V = 7.0 \text{ m/s}$, the pressure amplitude is 103,000 Pa, and at $V = 10.5 \text{ m/s}$ the pressure amplitude is 104419Pa.

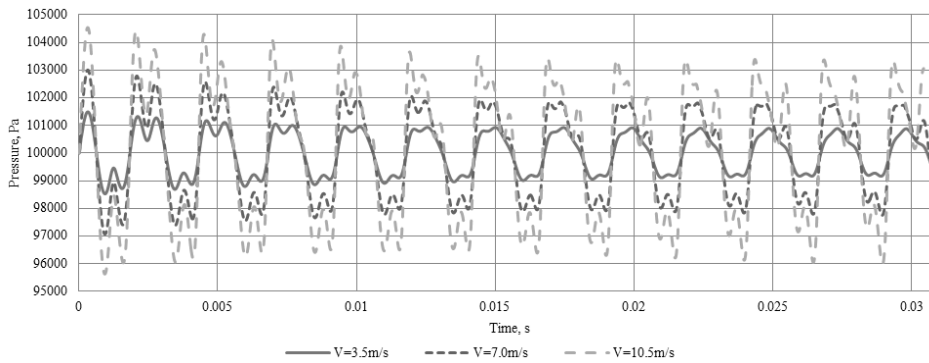


Fig.4. Pressure dependence in the gas-dynamic gap near the LS on time for different elasticity moduli of LS material.

Table 3. Pressure amplitude at LS different kinematic parameters.

Computational experiment	1	2	3
Propagation speed of gas oscillations in the LS circumferential direction, m/s	3.5	7.0	10.5
Maximum pressure amplitude U_p , MPa	0.101	0.103	0.104

When studying the temperature dependence of the gas dynamic cavity in the LS on kinematic parameters, the propagation speed of the gas oscillations in the circumferential direction varied and assumed values of 3.5, 7.0 or 10.5 m/s, the working fluid of the gas-dynamic cavity is air, adiabatic index is 1.4, air density $\rho = 1, 29 \text{ kg/m}^3$.

With speed increase from 3.5 m/s to 10.5 m/s oscillations in the temperature of the gas-dynamic cavity are observed, which have a periodic character (Fig. 5). The temperature amplitude is 271.9472K at $V = 3.5$ m/s. At $V = 7.0$ m/s the temperature amplitude is 275.1519 K, and at $V = 10.5$ m/s the temperature amplitude is 279.8211K.

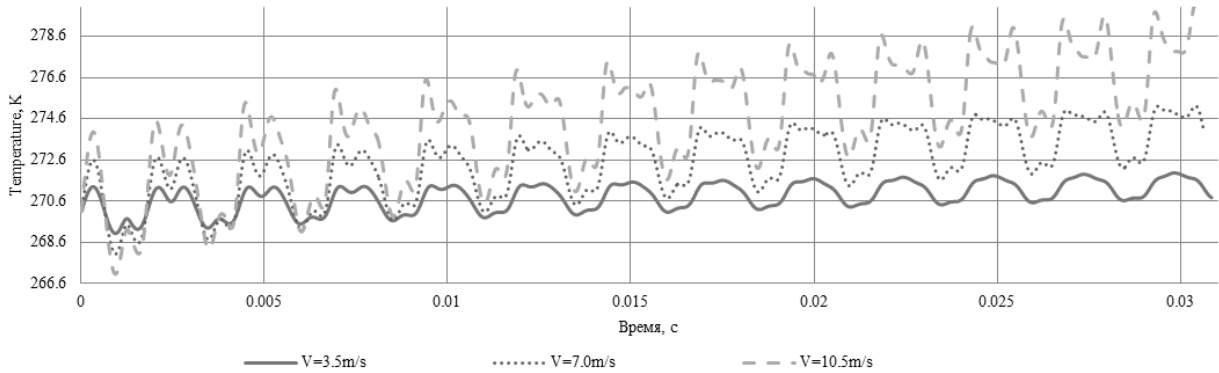


Fig.5. Temperature dependence of the LS gas-dynamic gap on time for various kinematic parameters.

Table 4. Temperature amplitude for LS different kinematic parameters.

Computational experiment	1	2	3
Propagation speed of gas oscillations in the LS circumferential direction, m/s	3.5	7.0	10.5
Temperature amplitude U_T , K	271.9472	275.1519	279.8211

5.3. Analysis of the influence of the working fluid characteristics

When studying the dependence of pressure oscillations in the LS gas-dynamic cavity on the working fluid characteristics the adiabatic index varied and was 1.1, 1.25 or 1.4 at density $\rho = 1,29 \text{ kg/m}^3$.

With an increase in the adiabatic index from 1.1 to 1.4, the pressure oscillations of the gas-dynamic cavity are observed, which have a periodic character (Fig. 6). The pressure amplitude is 102880.5 Pa for $k = 1.1$. For $k = 1.25$, the pressure amplitude is 102816.3 Pa, and for $k = 1.4$ the pressure amplitude is 1003003Pa.

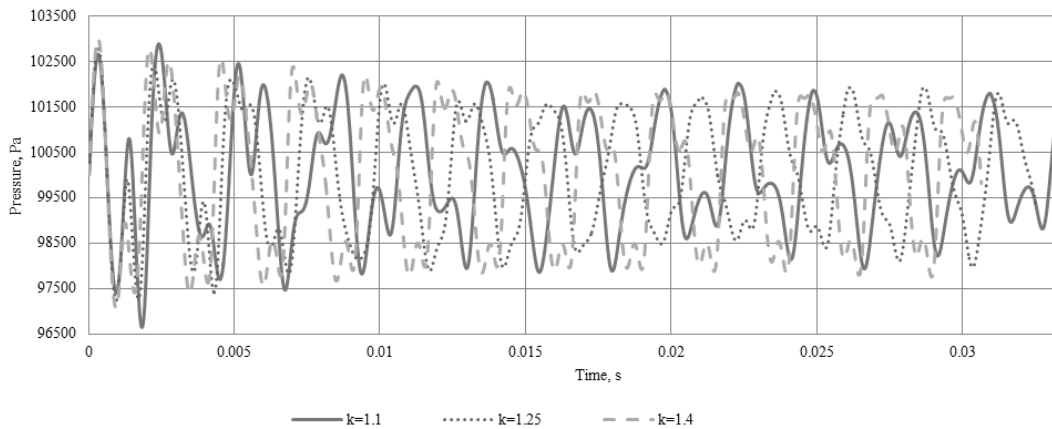


Fig.6. Pressure dependence of the LS gas-dynamic gap on time for different working fluid characteristics.

Table 5. Pressure amplitude for LS different working fluid characteristics.

Computational experiment	1	2	3
Adiabatic index, k	1.1	1.25	1.4
Maximum pressure amplitude U_P , MPa	0.103	0.103	0.1

When studying the dependence of temperature oscillations in the LS gas-dynamic cavity on the working fluid characteristics the adiabatic index varied and was 1.1, 1.25 or 1.4, with density $\rho = 1,29 \text{ kg/m}^3$.

With an increase in the adiabatic index from 1.1 to 1.4, the temperature oscillations of the gas-dynamic cavity are observed, which have a periodic character (Fig. 7). The temperature amplitude is 271.8515 K for $k = 1.1$. For $k = 1.25$ the temperature amplitude is 274.0991K, and for $k = 1.4$ the temperature amplitude is 275.1212K.

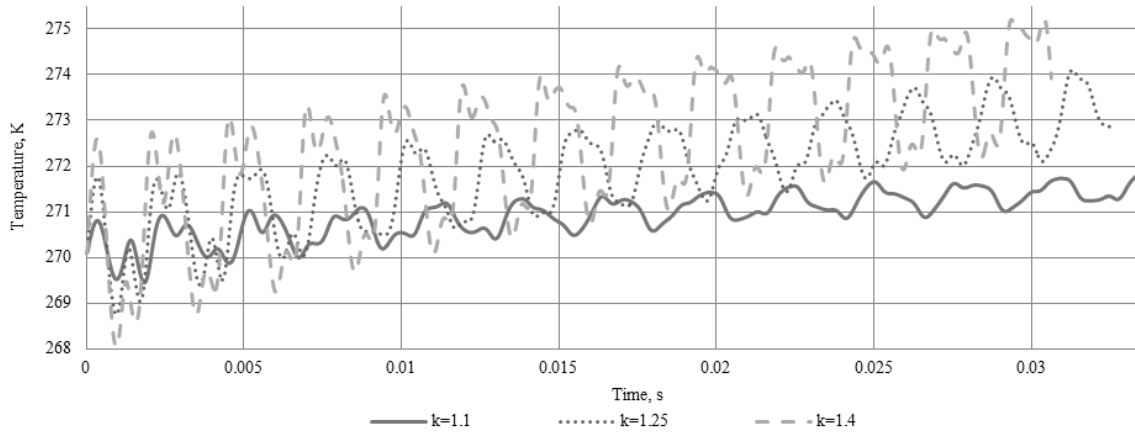


Fig.7. Temperature dependence of the LS gas-dynamic gap on time for different working fluid characteristics.

Table 6. Temperature amplitude for LS different kinematic parameters.

Computational experiment	1	2	3
Adiabatic index, k	1.1	1.25	1.4
Temperature amplitude U_T , K	271.8515	274.0991	275.1212

5.4. Analysis of the influence of physical and mechanical characteristics

In the bi-directional aeroelastic formulation the LS calculation scheme was generated (Fig. 8) and a solution was obtained using equations (1-9) and initial and boundary conditions, which allowed obtaining the following results.

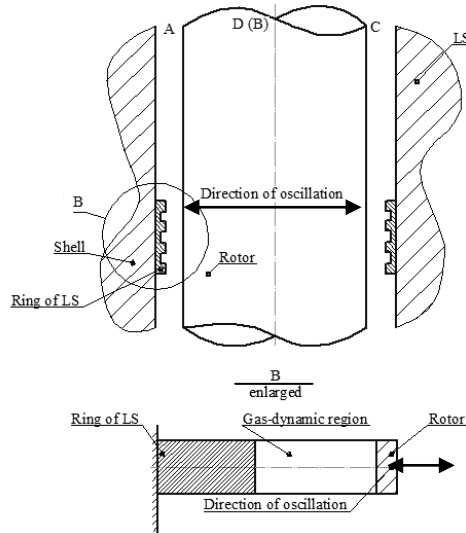


Fig. 8. Formation of the LS calculation scheme (bidirectional FSI-statement)

When studying the dependence of pressure oscillations in the LS gas-dynamic cavity on physico-mechanical characteristics of the LS the material density was set $\rho = 7800 \text{ kg/m}^3$, Poisson ratio $\mu = 0.35$, the elasticity modulus ranged within 50, 100, 150, 200 GPa. With an increase in elasticity modulus from 50 GPa to 200 GPa, the amplitude of the periodic pressure oscillations of the gas dynamic cavity decreases by 5 times. The pressure amplitude is 1 MPa at $E = 50 \text{ GPa}$. At $E = 100 \text{ GPa}$ the pressure amplitude is 0.5 MPa, and at $E = 150 \text{ GPa}$ the pressure amplitude is 0.3 MPa, at $E = 200 \text{ GPa}$ the pressure amplitude is 0.2 MPa (Fig. 9). Fig. 9 shows the dependence of pressure oscillations in the LS gas-dynamic gap on time for LS various physico-mechanical characteristics.

When studying the dependence of displacements in the LS structure on physico-mechanical characteristics the density of the LS material was set $\rho = 7800 \text{ kg/m}^3$, poisson ratio $\mu = 0.35$, adiabatic index $k = 1.4$, air density $\rho = 1.29 \text{ kg/m}^3$, $P_0 = 0.1 \text{ MPa}$, the calculated ratio of cells in the structure to the total number of cells calculated $FL = 0.96$, the elastic modulus varied within 50, 100, 150 and 200 GPa. Near the gas-dynamic gap with an increase in E from 50 GPa to 200 GPa oscillations of displacements in the LS structure are observed. The oscillations are periodic in nature and stable in time. The displacement amplitude is 1×10^{-2} microns at $E = 50 \text{ GPa}$. When $E = 100 \text{ GPa}$ the displacement amplitude is $5 \times 10^{-3} \text{ m}$, and when $E = 150 \text{ GPa}$ the displacement amplitude is $3 \times 10^{-3} \text{ m}$, for $E = 200 \text{ GPa}$ the displacement amplitude is $2.3 \times 10^{-3} \text{ m}$ (Fig.10). Figure 11 shows the relationship of displacements in the LS structure versus time for LS different physico-mechanical characteristics.

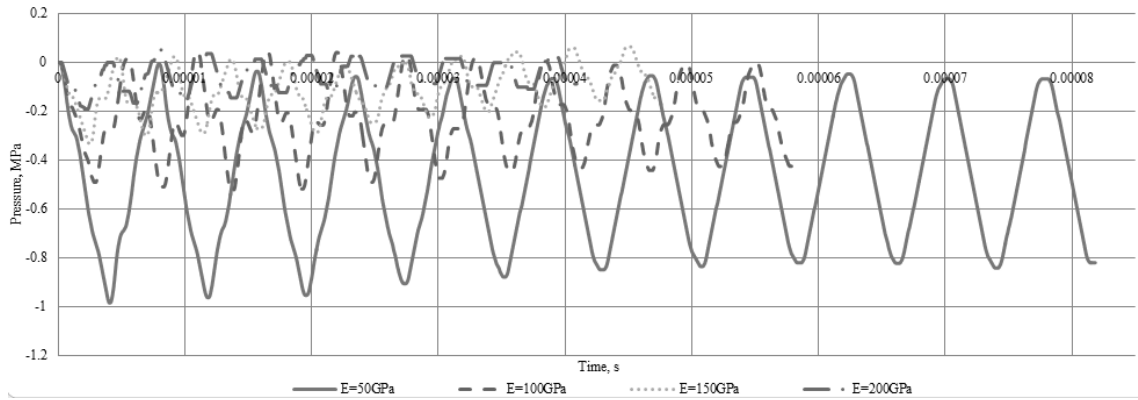


Fig. 9. Dependence of pressure oscillations in the LS gas-dynamic gap on time for LS various physico-mechanical characteristics.

Table 7. Amplitude of pressure oscillations at different values of LS physico-mechanical characteristics.

Computational experiment	1	2	3	4
Elasticity modulus E, GPa	50	100	150	200
Pressure amplitude U_p , MPa	1	0.5	0.3	0.2

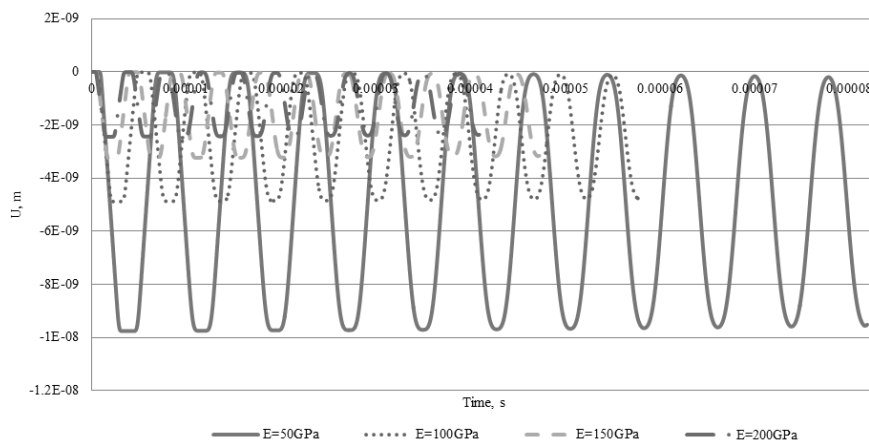


Fig. 10. Dependence of displacements in the LS structure versus time for LS various physico-mechanical characteristics.

Table 8. Displacements in the LS structure for LS different physico-mechanical characteristics.

Computational experiment	1	2	3	4
Elasticity modulus E, GPa	50	100	150	200
Displacement amplitude U_A , m	1×10^{-2}	5×10^{-3}	3×10^{-3}	2.3×10^{-3}

6. Conclusions

1. With an increase in the compression wave velocity arising from the approach of the rotor to the surface of the LS under vibrations from 3.5 m/s to 10.5 m/s the amplitude of the gas dynamic force increases from 23.6H to 45.5H. The frequency does not change and is equal to 400 Hz. At a natural rotor frequency of 808 Hz, one can expect that with a minimum value of the gas flow velocity in the circumferential direction, weak vibrations may appear. As the speed increases, one can expect an increase in the LS vibrations.

2. With the shaft diameter increase from 65mm to 260mm, the maximum amplitude of the gas dynamic force of 82.7N is observed at a diameter equal to 130 mm, the minimum amplitude of the gas dynamic force is observed at a diameter of 65mm from 7.7H, the frequency is 400Hz. The maximum frequency of the gas dynamic force is 770 Hz with a diameter of 65 mm. The minimum frequency of the gas-dynamic force is 406 Hz with the diameter equal to 260 mm. It can be seen that as the rotor diameter increases, the nominal values of the gas dynamic force increase. This is due to the increase in the rotor area at a constant nominal pressure. In this case the maximum amplitudes of gas-dynamic forces are observed when the oscillation frequency f_p of the rotor is equal to the first natural frequency of the gas-dynamic pressure fluctuations of the circumferential cavity in the gap. Oscillation amplitude of gas-dynamic forces are lower at the rotor oscillation frequency f_p equal to the second natural frequency of the gas-dynamic pressure oscillations of the circumferential cavity in the gap. Even lower are the amplitudes of gas-dynamic force oscillations at the rotor oscillation frequency f_p equal to the fourth natural frequency of the circumferential pressure oscillations of the gas-dynamic cavity in the gap. The oscillation amplitude of the gas-dynamic forces was also low at the natural frequency of the gas-dynamic cavity nonmultiple for the rotor frequency.

3. With an increase in the adiabatic index k from 1.1 to 1.4 the gas-dynamic force oscillation amplitude increases from 29.63N to 35.15N, and the oscillation frequency of gas-dynamic forces decreases from 392Hz to 388Hz. Thus, we note a weak influence of the working fluid characteristics on the LS vibrations.

4. With increase in elastic modulus from 50GPa to 200GPa the pressure oscillation amplitude decreases from 0.97MPa to 0.19MPa, pressure oscillation frequency rises from 134kHz to 256kHz. Analysis of the influence of physical and mechanical characteristics on the LS vibrations demonstrated that with a hard material the strain rate is lower than with a soft material. The displacements in a softer material under given loads are 1×10^{-2} microns. In a harder material the displacement amplitude is much lower.

5. By changing the rotor diameter, it is possible to reduce vibration. Thus, it is possible to reduce the gaps in the LS and reduce leakage.

Acknowledgements

The study was performed with a grant from the Russian Science Foundation (project №14-19-00877).

References

- [1] Butymova LN. Effect of vibration on gas dynamics in modeling labyrinth seals of a gas transmittal unit centrifugal compressor. *Bulletin of Perm National Research Polytechnic University. Aerospace technology* 2016; 47: 243–259.
- [2] Butymova LN, Modorsky VY, Petrov VY. Numerical modeling of the dynamic interaction in system "gas-structure" with harmonic motion of the piston in the variable section pipe. *AIP Conference Proceedings* 2016; 1770: 030103-1–030103-5.
- [3] Butymova LN, Modorskii VY. One-way FSI simulation of the phase and the geometric parameters of the model of compressor blades on the oscillating gas-dynamic processes pipe. *MATEC the Web Conf.* 2016; 75: 4 p.
- [4] Butymova LN, Modorsky VY, Petrov VY. Numerical modeling the kinematic parameter effect on the vibrations of the model compressor vanes in the system "gas-structure". *Scientific and Technical Gazette Volga region* 2015; 5: 157–160.
- [5] Butymova LN, Modorsky VY, Shmakov AF. Experimental estimation of amplitude and phase characteristics of the interaction of gas-dynamic flow and structure. *Scientific and Technical Gazette Volga Region* 2014; 5: 127–129.
- [6] Butymova LN, Modorsky VY. Investigation of gas-dynamic flow and structure in a model experimental setup. *Bulletin of South Ural State University. Series: Computational Mathematics and Computer Science-* 2014; 3(2): 92–100.
- [7] Butymova LN, Modorsky VY. Study of oscillatory processes on resonant modes in the model apparatus. *Scientific and Technical Gazette Volga region* 2013; 6: 193–196.
- [8] Butymova LN, Modorsky VY, Sokolkin YV. Development of experimental apparatus and investigation of the body material influence on the resonance frequencies in the "gas-structure". *Scientific and Technical Gazette Volga Region* 2013; 6: 197–200.
- [9] Mekhonoshina EV, Modorsky VY. Development of numerical simulation techniques of the compressor aeroelastic operation. *Scientific and Technical Gazette Volga Region* 2014; 5: 264–268.
- [10] Mekhonoshina EV, Modorsky VY. Impact of magnetic suspension stiffness on aeroelastic compressor rotor vibrations of gas pumping units. *AIP Conference Proceedings* 2016; 1770: 030113-1–030113-5.
- [11] Makarov AA, Zaytsev NN. Engineering and theoretical problems of labyrinth seal applications in high-speed rotary machines. *Herald PNRPU. Aerospace engineering* 2015; 42: 61–81.
- [12] Brikin BV, Evdokimov IE. Numerical simulation of the experiment on the flow in the labyrinth seal. *Proceedings of the MAI # 61*. URL: [http://mai.ru/science/trudy/published.php\(02/02/2017\)](http://mai.ru/science/trudy/published.php(02/02/2017)).
- [13] Arbuzov IA, Tashkinov AA, Schenyatsky DV, Kirievsky BE, Bulbovich RV, Modorsky VY, Pisarev PV. Analysis of the impact of the entry apparatus in the connecting channel on the vibrational processes in the first stage of two-stage model pump. *Scientific and Technical Gazette Volga* 2012; 6: 108–111.
- [14] Gaynutdinova DF, Modorsky VY, Shevelev NA. Experimental modeling of cavitation occurring at vibration. *AIP Conference Proceedings* 2016; 1770: 030111-1–030111-4.
- [15] Shmakov AF, Modorsky VY. Numerical simulation of gas-dynamic, thermal processes and evaluation of the stress-strain state in the modeling compressor of the gas-distributing unit. *AIP Conference Proceedings* 2016; 1770: 030108-1–030108-5.
- [16] Babushkina AV, Modorsky VY, Sipatov AM, Kolodyazhny DY, Nagorny VS. Modeling technique for the process of liquid film disintegration. *AIP Conference Proceedings* 2016; 1770: 030109-1–030109-7.
- [17] Kalyulin SL, Modorsky VY, Paduchev AP. Numerical design of the rectifying lattices in a small-sized wind tunnel. *AIP Conference Proceedings* 2016; 1770: 030110-1–030110-4.
- [18] Modorsky VY, Shevelev NA. Research of aerohydrodynamic and aeroelastic processes on PNRPU HPC system. *AIP Conference Proceedings* 2016; 1770: 030110-1–030110-4.
- [19] Modorsky VY et al. Numerical study of actual problems of mechanical engineering and mechanics of solid and bulk materials by large particles method. A study of actual problems of mechanics and engineering. Moscow: National Academy of Applied Sciences, International Association of developers and users of the method of large particles 1995; 5: 1658 p.
- [20] Modorsky VY, Shmakov AF, Butymova LN, Gainutdinova DF, Mekhonoshina EV, Kalyulin SL. Parallel calculation of dynamic processes in large-sized supercharger. *Scientific service on the Internet: A variety of supercomputing worlds Proceedings of the International Supercomputer Conference. Russian Academy of Sciences Supercomputing Consortium of Russian Universities* 2014: 258–262.
- [21] Shmakov AF, Modorsky VY. Energy Conservation in Cooling Systems at Metallurgical Plants. *Metallurgist* 2016; 59(9): 882–886.
- [22] Mekhonoshina EV, Modorskii VY. On a phase-shift of waves at the medium interface. *Computer Optics* 2015; 39(3): 385–391. DOI: 10.18287/0134-2452-2015-39-3-385-391.